Electronic Supplementary Material (ESI) for Dalton Transactions.

Bright Luminescence in Lanthanide Coordination Polymers with Tetrafluoroterephthalate as a Bridging Ligand

Miriam Sobieray, Jens Gode, Christiane Seidel, Marieke Poß, Claus Feldmann, and Uwe Ruschewitz

Contents:

$^{2}_{\infty}$[Ln^{III}(tfBDC)(NO_3)($DMF)_2$]·DMF with Ln^{3+} = Eu (**1**), Gd (**2**), Tb (**3**), Ho (**4**), Tm (**5**)

$^{2}_{\infty}$[Ln^{III}(tfBDC)(CH_3COO)($FA)_3$]·3FA with Ln^{3+} = Sm (**6**), Eu (**7**)

$^{2}_{\infty}$[Ln^{III}(tfBDC)(NO_3)($DMSO)_2$] with Ln^{3+} = Ho (**8**), Er (**9**), Tm (**10**)

Figures S1 - S5: XRPD patterns of **1** – **5**.

Figures S6 - S9: DTA/TG curves of **1**, **2**, **4**, **5**.

Figure S10: IR spectra of **1** – **5**.

Table S1: Summary of IR data of **1** – **3**.

Figures S11 - S12: XRPD patterns of **6**, **7**.

Figures S13 - S14: DTA/TG curves of **6**, **7**.

Figure S15: IR spectra of **6**, **7**.

Table S2: Summary of IR data of **6**, **7**.

Figures S16 - S18: XRPD patterns of **8** – **10**.

Figures S19 - S20: DTA/TG curves of **9** – **10**.

Figure S21: IR spectra of **8** – **10**.

Table S3: Summary of IR data of **8** – **10**.

Figure S22: Dimeric units in **1**.

Figure S23: View of a polymeric layer in the crystal structure of **1**.

Figure S24: View of a polymeric layer in the crystal structure of **10** in a space-filling presentation.

Figures S25-S27: Excitation spectra of **1**, **3**, and **7**.

Figure S28: Comparison of excitation spectra of **1** and **7**.

Figure S29: Comparison of emission spectra of **1** and **7**.

Figure S30: XRPD of the residue of **9** after heating at 500 °C.

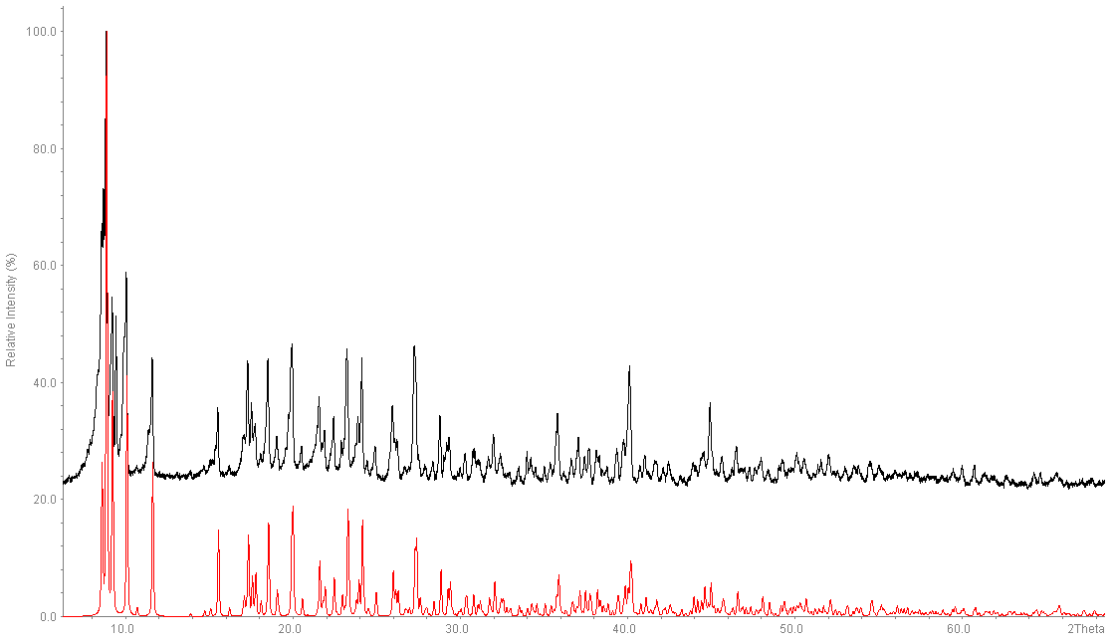

Figure S1: X-ray powder diffraction pattern (Huber G670, CuKα_1 radiation, flat sample, 12 h) of $^{2}_{\infty}$[Eu^{III}(tfBDC)(NO$_3$)(DMF)$_2$]·DMF (**1**, black) compared to a theoretical pattern calculated from single crystal structure data (red) (reflections at 2θ ≈ 21.5° and 23.7° originate from the foil of the sample holder).

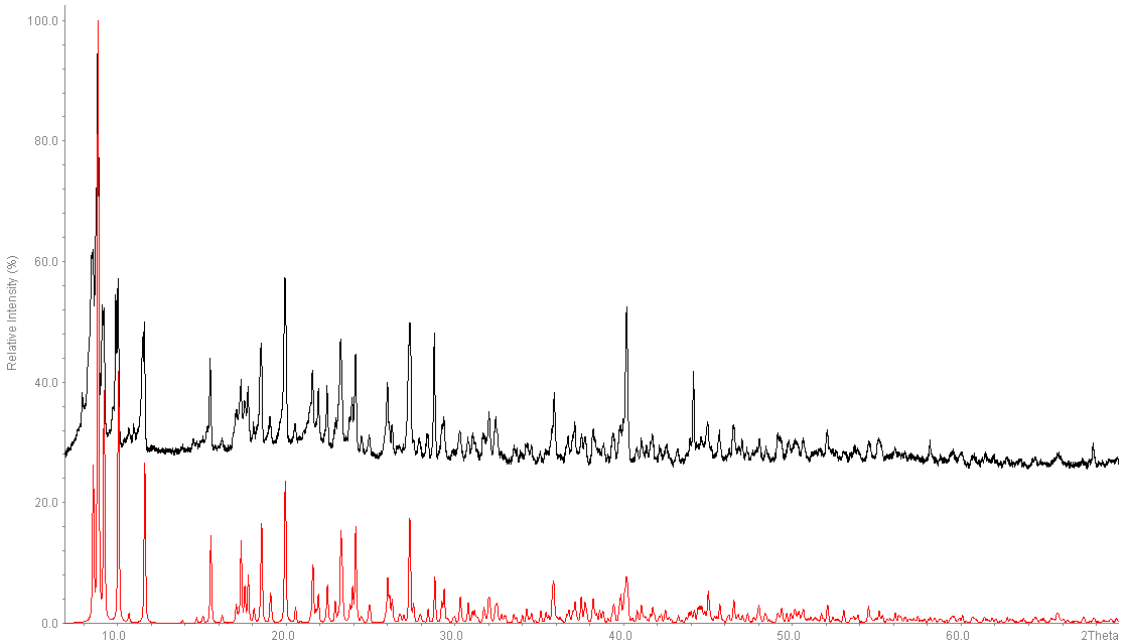

Figure S2: X-ray powder diffraction pattern (Huber G670, CuKα_1 radiation, flat sample, 12 h) of $^{2}_{\infty}$[Gd^{III}(tfBDC)(NO$_3$)(DMF)$_2$]·DMF (**2**, black) compared to a theoretical pattern calculated from single crystal structure data (red) (reflections at 2θ ≈ 21.5° and 23.7° originate from the foil of the sample holder).

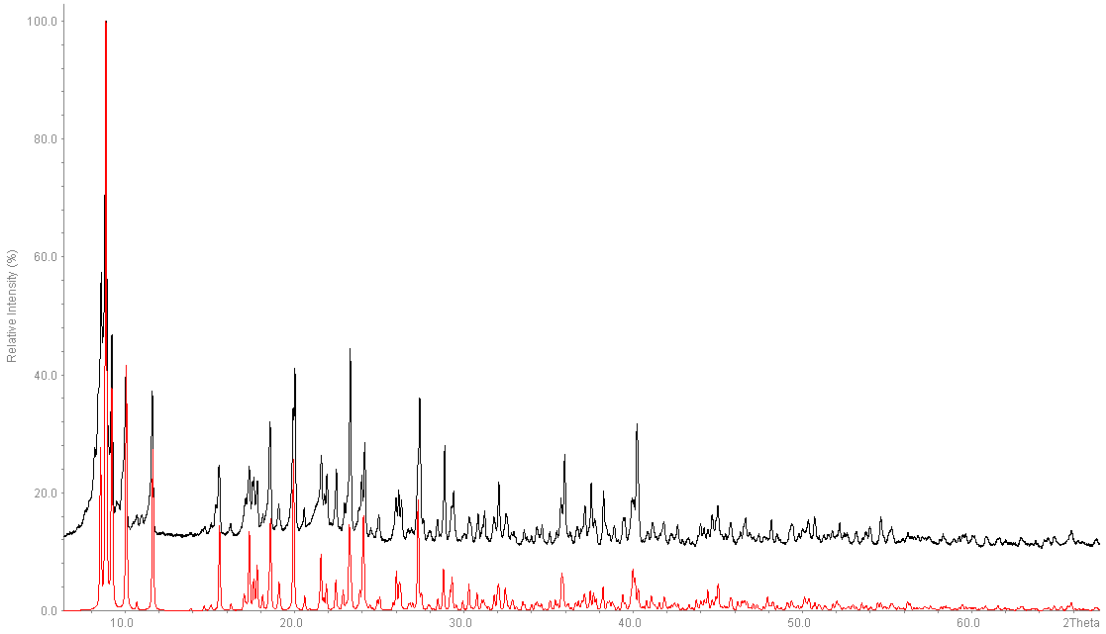

Figure S3: X-ray powder diffraction pattern (Huber G670, CuKα_1 radiation, flat sample, 12 h) of $^{2}_{\infty}$[Tb^{III}(tfBDC)(NO$_3$)(DMF)$_2$]·DMF (**3**, black) compared to a theoretical pattern calculated from single crystal structure data (red) (reflections at 2θ ≈ 21.5° and 23.7° originate from the foil of the sample holder).

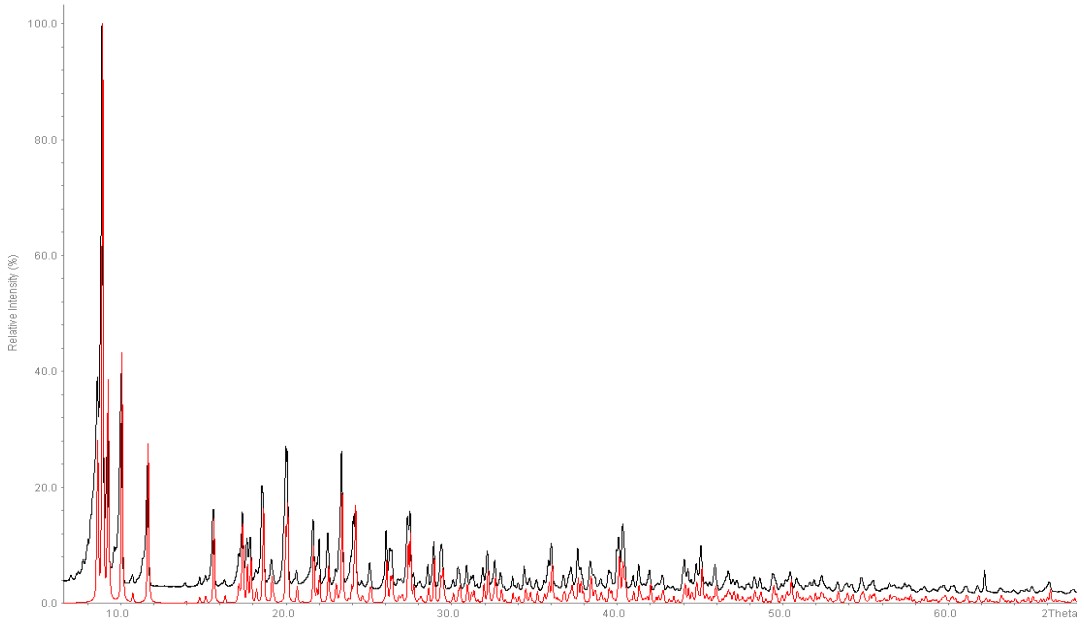

Figure S4: X-ray powder diffraction pattern (Huber G670, CuKα_1 radiation, flat sample, 12 h) of $^{2}_{\infty}$[Ho^{III}(tfBDC)(NO$_3$)(DMF)$_2$]·DMF (**4**, black) compared to a theoretical pattern calculated from single crystal structure data (red) (reflections at 2θ ≈ 21.5° and 23.7° originate from the foil of the sample holder).

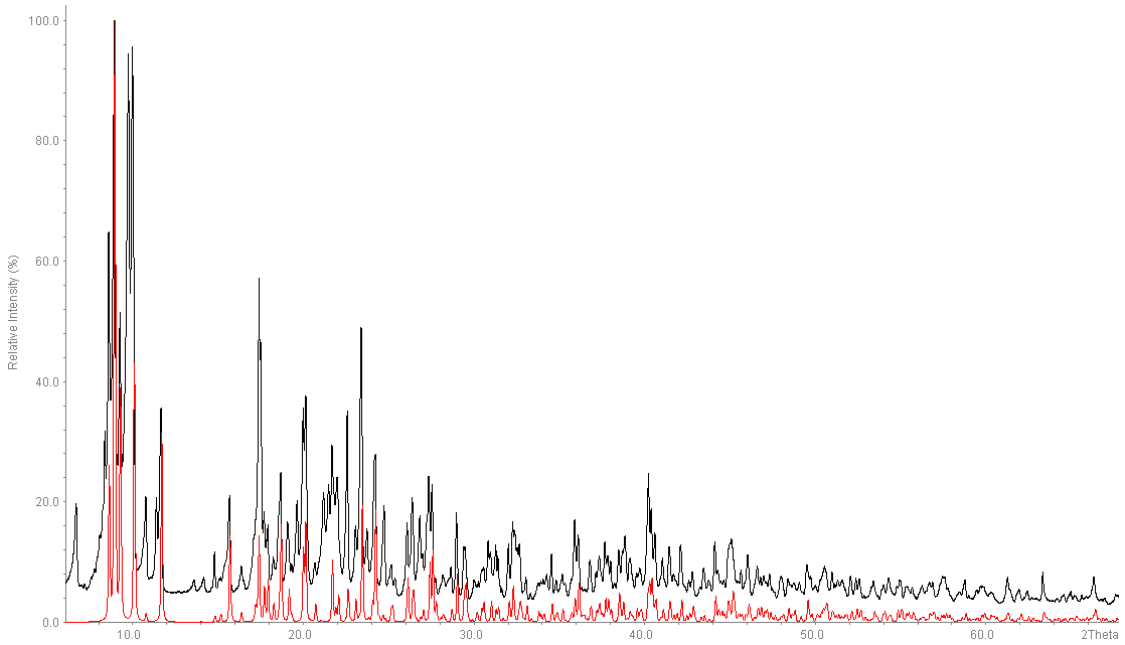

Figure S5: X-ray powder diffraction pattern (Huber G670, CuKα_1 radiation, flat sample, 12 h) of $^{2}_{\infty}$[Tm^{III}(tfBDC)(NO$_3$)(DMF)$_2$]·DMF (**5**, black) compared to a theoretical pattern calculated from single crystal structure data (red) (reflections at 2θ ≈ 21.5° and 23.7° originate from the foil of the sample holder).

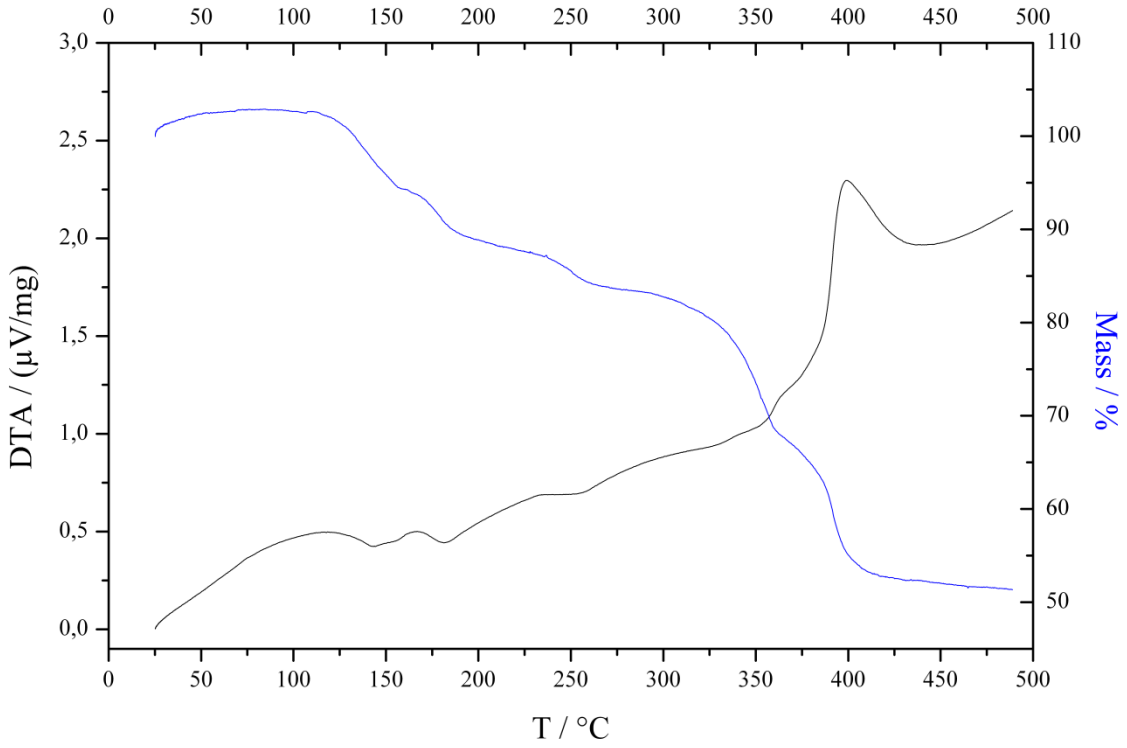

Figure S6: DTA (black) and TG (blue) curves of $^{2}_{\infty}$[Eu^{III}(tfBDC)(NO$_3$)(DMF)$_2$]·DMF (**1**).

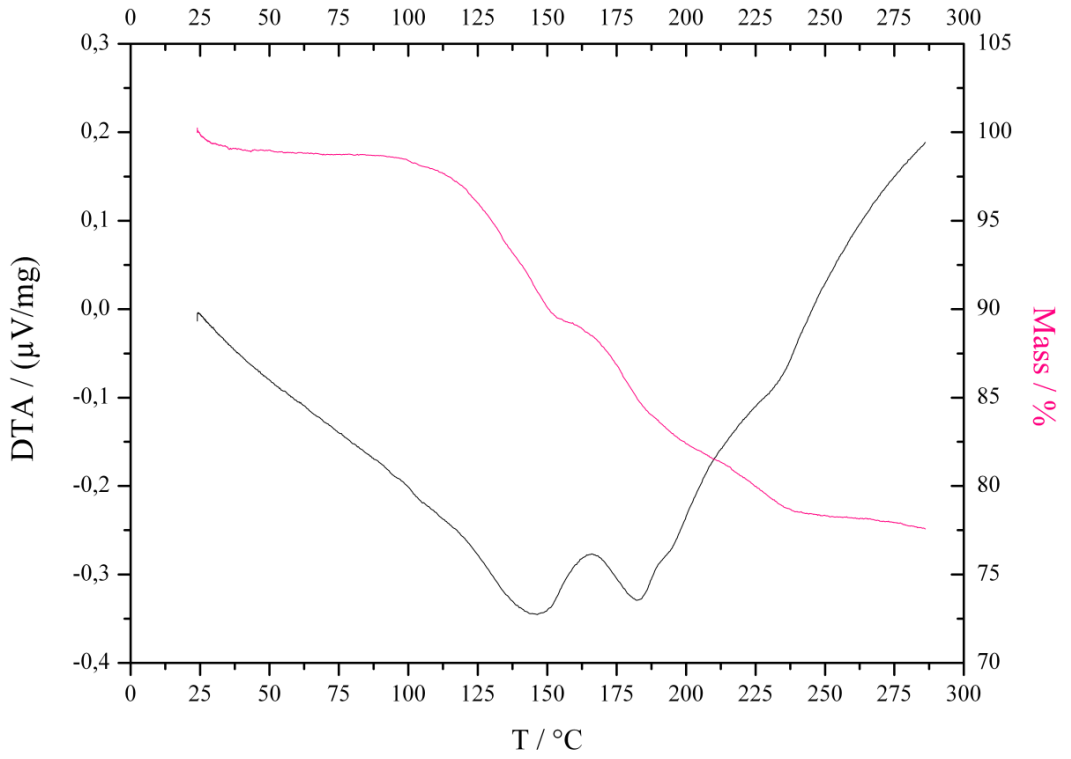

Figure S7: DTA (black) and TG (pink) curves of $^{2}_{\infty}[Gd^{III}(tfBDC)(NO_3)(DMF)_2]\cdot DMF$ (**2**).

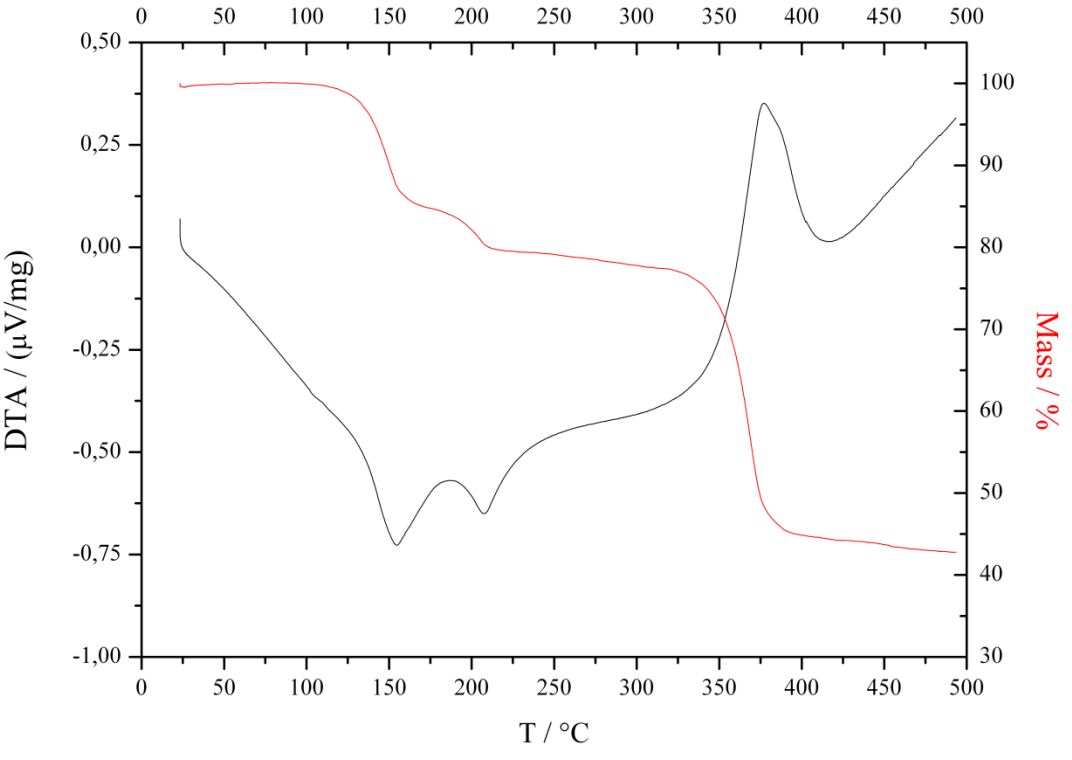

Figure S8: DTA (black) and TG (red) curves of $^{2}_{\infty}[Ho^{III}(tfBDC)(NO_3)(DMF)_2]\cdot DMF$ (**4**).

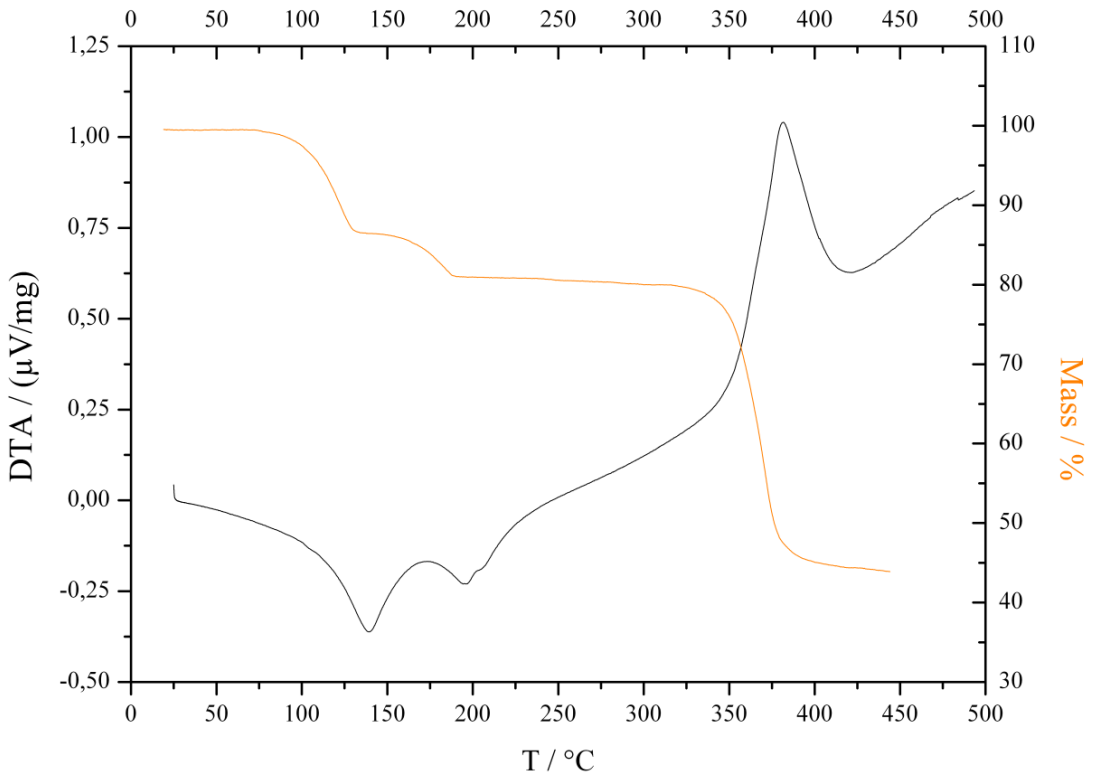

Figure S9: DTA (black) and TG (orange) curves of $^{2}_{\infty}[Tm^{III}(tfBDC)(NO_3)(DMF)_2]\cdot DMF$ (**5**).

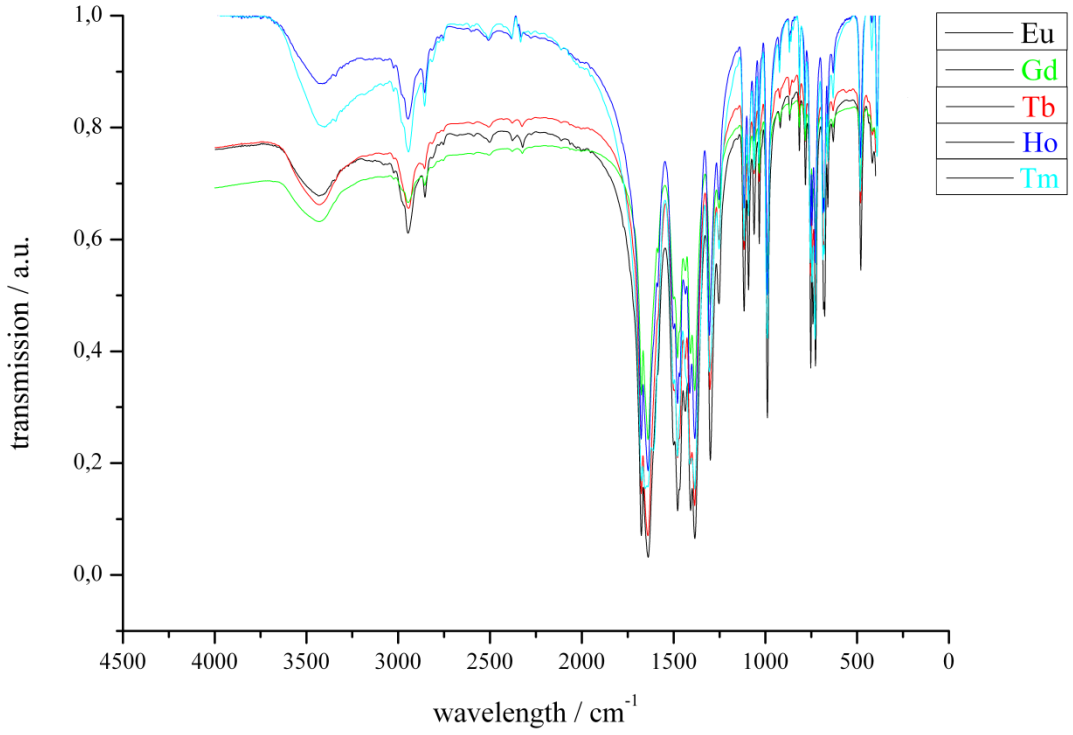

Figure S10: IR spectra of compounds **1 - 5**.

Table S1: Summary of IR data of **1 - 3**.

1	IR (KBr, cm^{-1}): 3429 (b), 3025 (w), 2964 (m), 2853 (w), 2811 (w), 2775 (w), 2755 (w), 2586 (w), 2504 (w), 2379 (w), 2324 (w), 2115 (w), 2064 (w), 2032 (w), 2004 (w), 1984 (w), 1954 (w), 1676 (s), 1639 (s), 1585 (m), 1501 (m), 1479 (s), 1469 (w), 1437 (m), 1409 (s), 1384 (s), 1300 (s), 1256 (m), 1117 (m), 1092 (m), 1062 (m), 1034 (m), 989 (s), 921 (w), 868 (w), 816 (w), 783 (w), 753 (s), 741 (s), 727 (s), 679 (s), 661 (m), 630 (w), 480 (m), 435 (w), 418 (w).
2	IR (KBr, cm^{-1}): 3429 (b), 3020 (w), 2982 (w), 2968 (w), 2947 (w), 2854 (w), 2815 (w), 2500 (w), 2376 (w), 2322 (w), 2324 (w), 1675 (s), 1639 (s), 1585 (w), 1500 (w), 1479 (s), 1468 (w), 1435 (w), 1408 (s), 1385 (s), 1300 (m), 1254 (w), 1115 (m), 1092 (m), 1063 (m), 1036 (m), 989 (m), 922 (w), 868 (w), 815 (w), 783 (w), 756 (m), 743 (s), 727 (s), 685 (s), 660 (m), 662 (m), 631 (w), 480 (m), 436 (w), 417 (w).
3	IR (KBr, cm^{-1}): 3427 (b), 3024 (w), 2945 (m), 2856 (w), 2815 (w), 2777 (w), 2756 (w), 2590 (w), 2507 (w), 2379 (w), 2324 (w), 2113 (w), 2067 (w), 2034 (w), 2006 (w), 1984 (w), 1956 (w), 1676 (s), 1641 (s), 1585 (m), 1500 (m), 1479 (s), 1467 (w), 1439 (m), 1409 (s), 1387 (s), 1302 (s), 1256 (m), 1117 (m), 1094 (m), 1063 (m), 1036 (m), 991 (s), 922 (w), 868 (w), 849 (w), 816 (w), 783 (w), 756 (s), 745 (s), 729 (s), 685 (s), 679 (s), 662 (m), 631 (w), 480 (m), 440 (w), 417 (w).

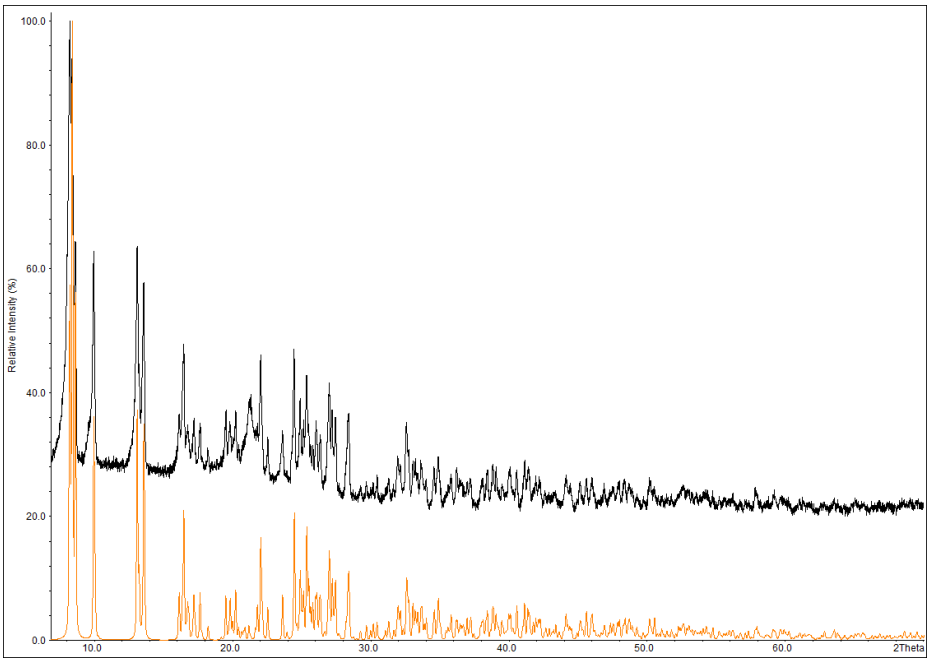

Figure S11: X-ray powder diffraction pattern (Huber G670, CuKα_1 radiation, flat sample, 60 min) of $^{2}_{\infty}$ [Sm^{III}(tfBDC)(CH_3COO)($HCONH_2$)$_3$]·3$HCONH_2$ (**6**, black) compared to a theoretical pattern calculated from single crystal structure data (orange) (reflections at 2θ ≈ 21.5° and 23.7° originate from the foil of the sample holder).

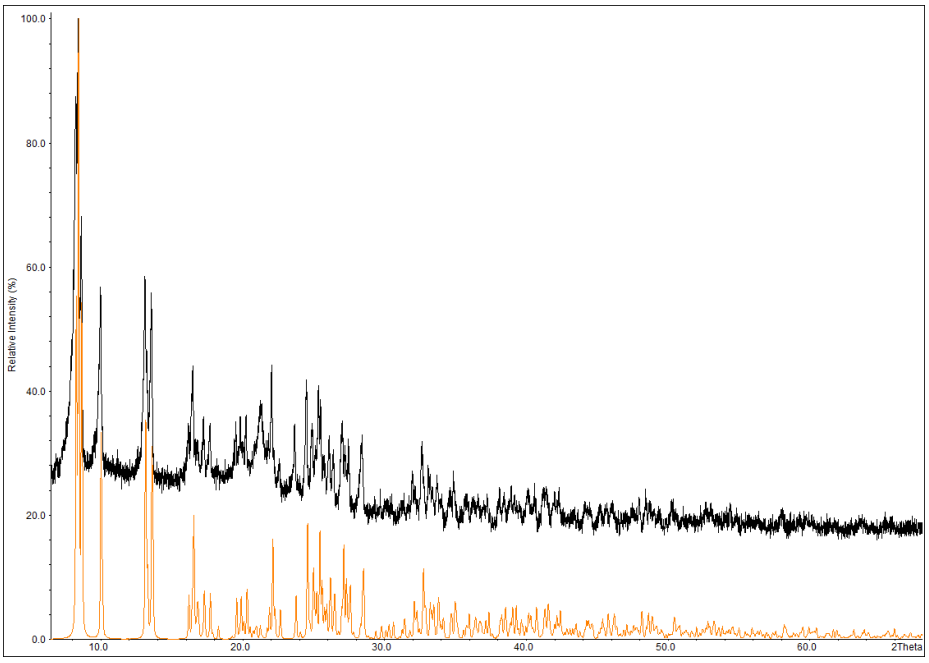

Figure S12: X-ray powder diffraction pattern (Huber G670, CuKα_1 radiation, flat sample, 60 min) of $^{2}_{\infty}$ [Eu^{III}(tfBDC)(CH_3COO)($HCONH_2$)$_3$]·3$HCONH_2$ (**7**, black) compared to a theoretical pattern calculated from single crystal structure data (orange) (reflections at 2θ ≈ 21.5° and 23.7° originate from the foil of the sample holder).

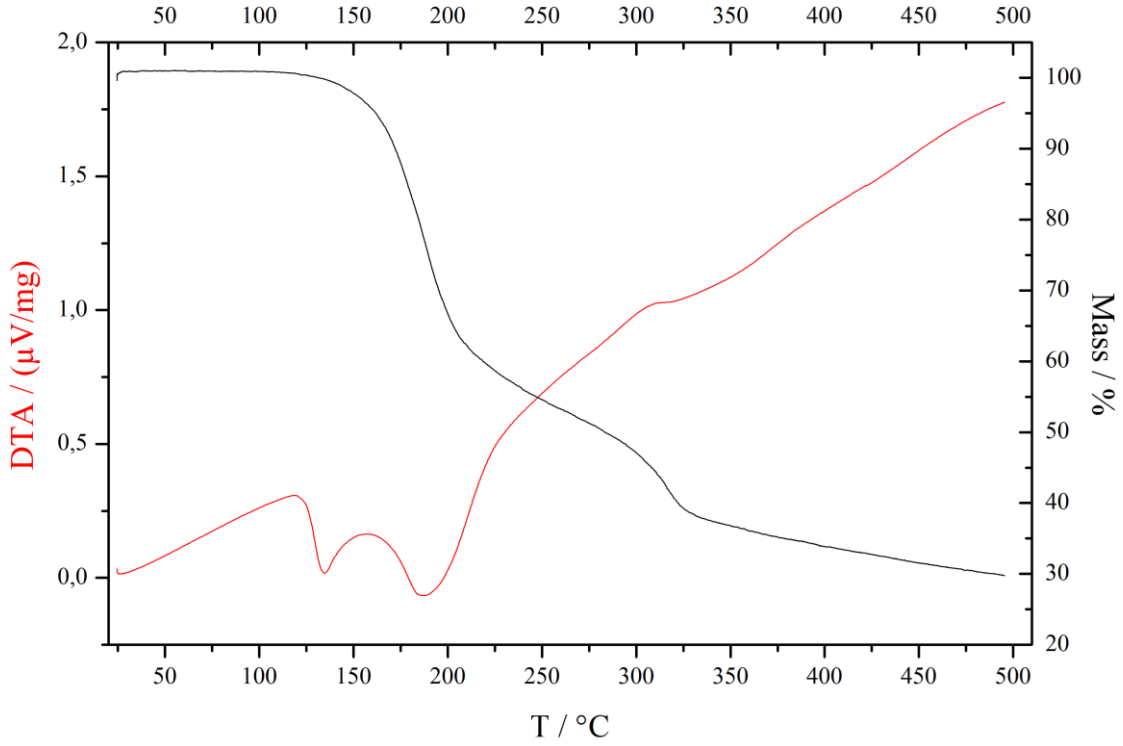

Figure S13: DTA (red) and TG (black) curves of $^{2}_{\infty}$ [Sm^{III}(tfBDC)(CH_3COO)($HCONH_2$)$_3$]·3$HCONH_2$ (**6**).

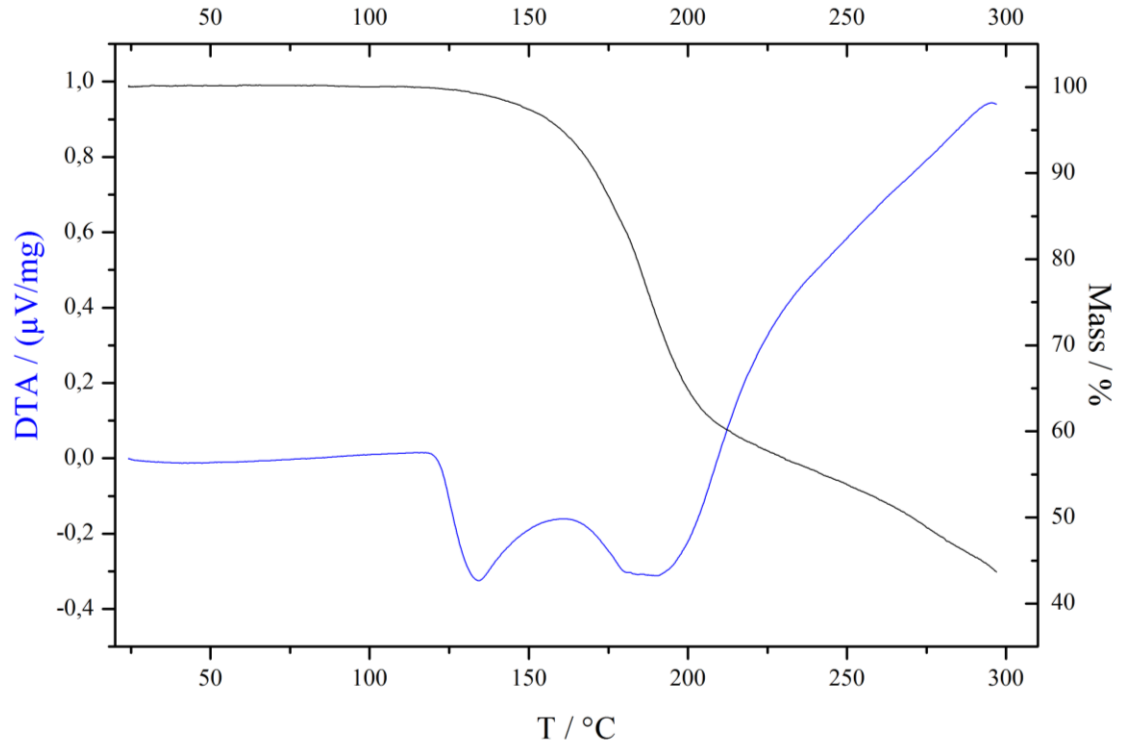

Figure S14: DTA (blue) and TG (black) curves of $^{2}_{\infty}$ [Eu^{III}(tfBDC)(CH_3COO)($HCONH_2$)$_3$]·3$HCONH_2$ (**7**).

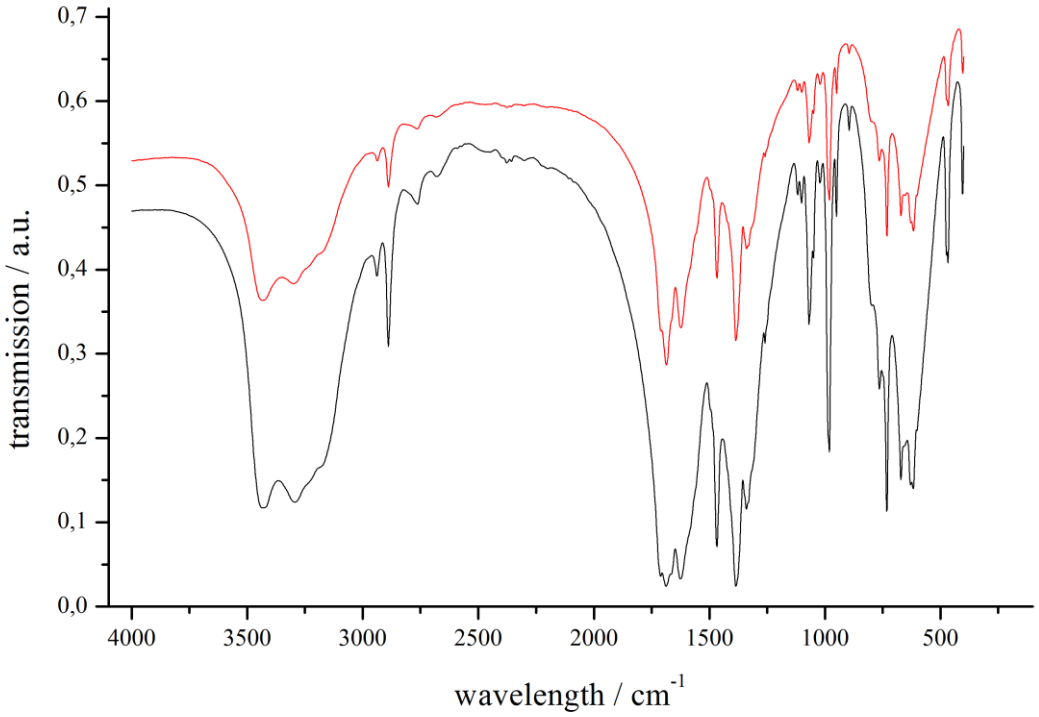

Figure S15: IR spectra of compounds **6** (Sm, red) and **7** (Eu, black).

Table S2: Summary of IR data of **6** and **7**.

6	IR (KBr, cm^{-1}): 3433(b), 3298 (b), 2937 (w), 2889 (s), 2767 (w), 2682 (b), 2378 (b), 1685 (w), 1623 (m), 1467 (s), 1384 (s), 1340 (w), 1330 (w), 1259 (w), 1118 (w), 1101 (w), 1068 (s), 1020 (b), 981 (s), 948 (s), 894 (w), 765 (b), 730 (s), 671 (m), 617 (b), 466 (m), 403 (m).
7	IR (KBr, cm^{-1}): 3433 (b), 3298 (b), 2937 (w), 2889 (s), 2767 (w), 2676 (b), 2376 (b), 1685 (w), 1625 (m), 1467 (s), 1384 (s), 1340 (m), 1259 (w), 1118 (w), 1101 (w), 1068 (s), 1049 (w), 1022 (b), 981 (s), 950 (s), 894 (w), 763 (b), 732 (s), 671 (m), 628 (b), 617 (b), 466 (m), 403 (m).

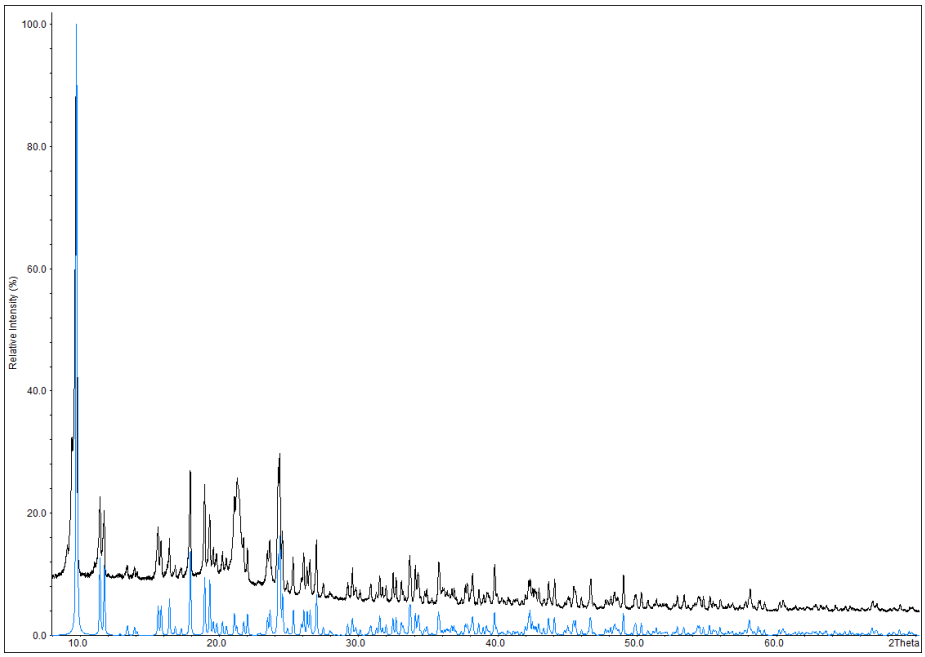

Figure S16: X-ray powder diffraction pattern (Huber G670, CuKα_1 radiation, flat sample, 60min) of $^{2}_{\infty}[Ho^{III}(tfBDC)(NO_3)(DMSO)_2]$ (**8**, black) compared to a theoretical pattern calculated from single crystal structure data (blue) (reflections at $2\theta \approx 21.5°$ and 23.7° originate from the foil of the sample holder).

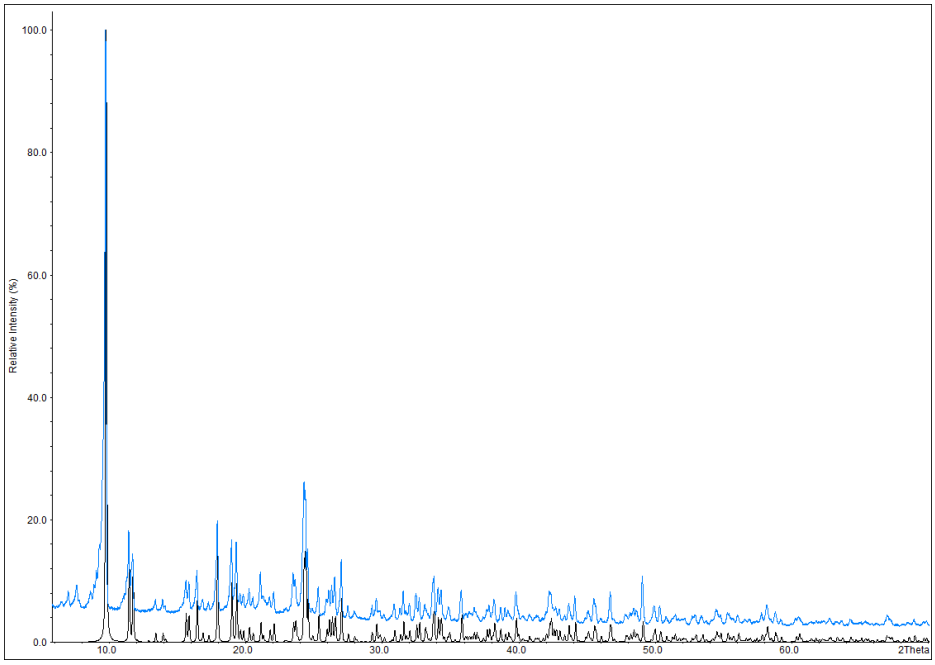

Figure S17: X-ray powder diffraction pattern (Huber G670, CuKα_1 radiation, flat sample, 60min) of $^{2}_{\infty}[Er^{III}(tfBDC)(NO_3)(DMSO)_2]$ (**9**, blue) compared to a theoretical pattern calculated from single crystal structure data (black) (reflections at $2\theta \approx 21.5°$ and 23.7° originate from the foil of the sample holder).

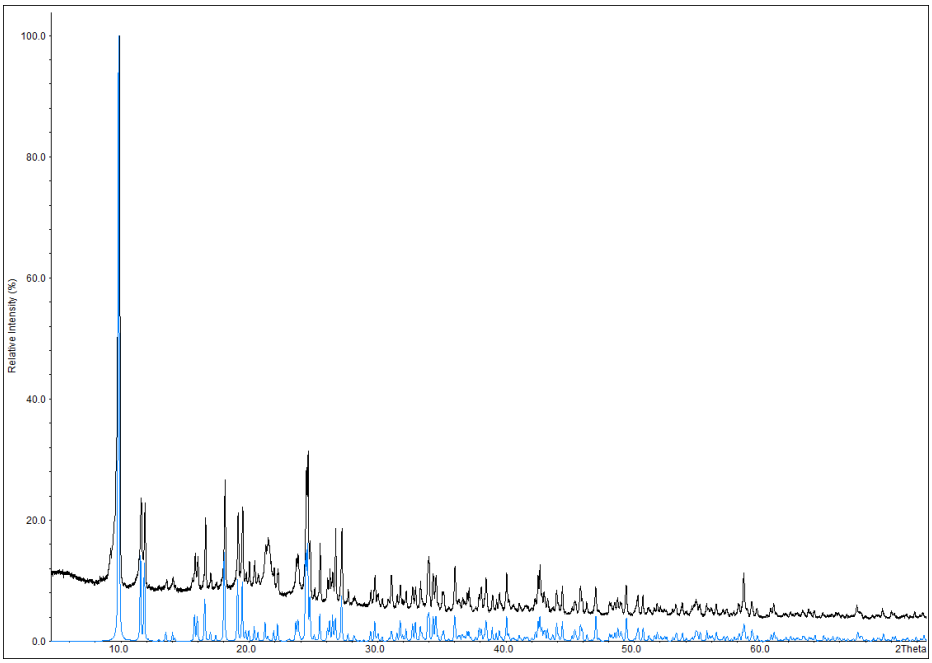

Figure S18: X-ray powder diffraction pattern (Huber G670, CuKα_1 radiation, flat sample, 120min) of $^{2}_{\infty}$[Tm^{III}(tfBDC)(NO$_3$)(DMSO)$_2$] (**10**, black) compared to a theoretical pattern calculated from single crystal structure data (blue) (reflections at $2\theta \approx 21.5°$ and 23.7° originate from the foil of the sample holder).

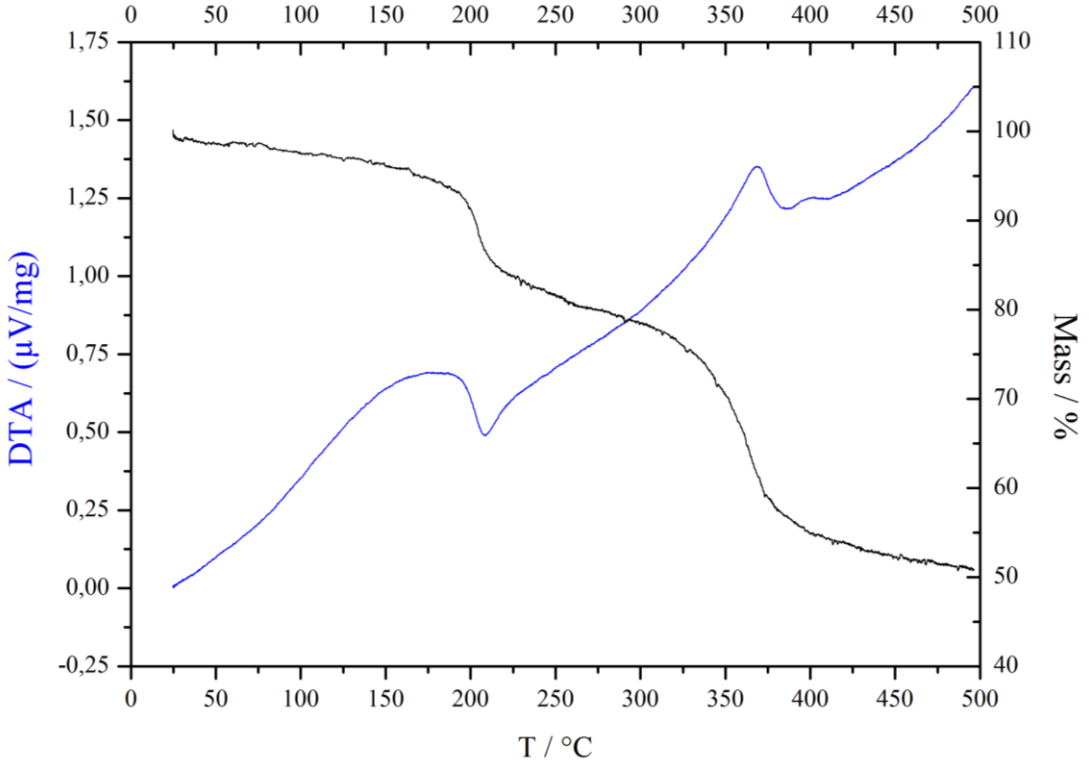

Figure S19: DTA (blue) and TG (black) curves of $^{2}_{\infty}$[Er^{III}(tfBDC)(NO$_3$)(DMSO)$_2$] (**9**).

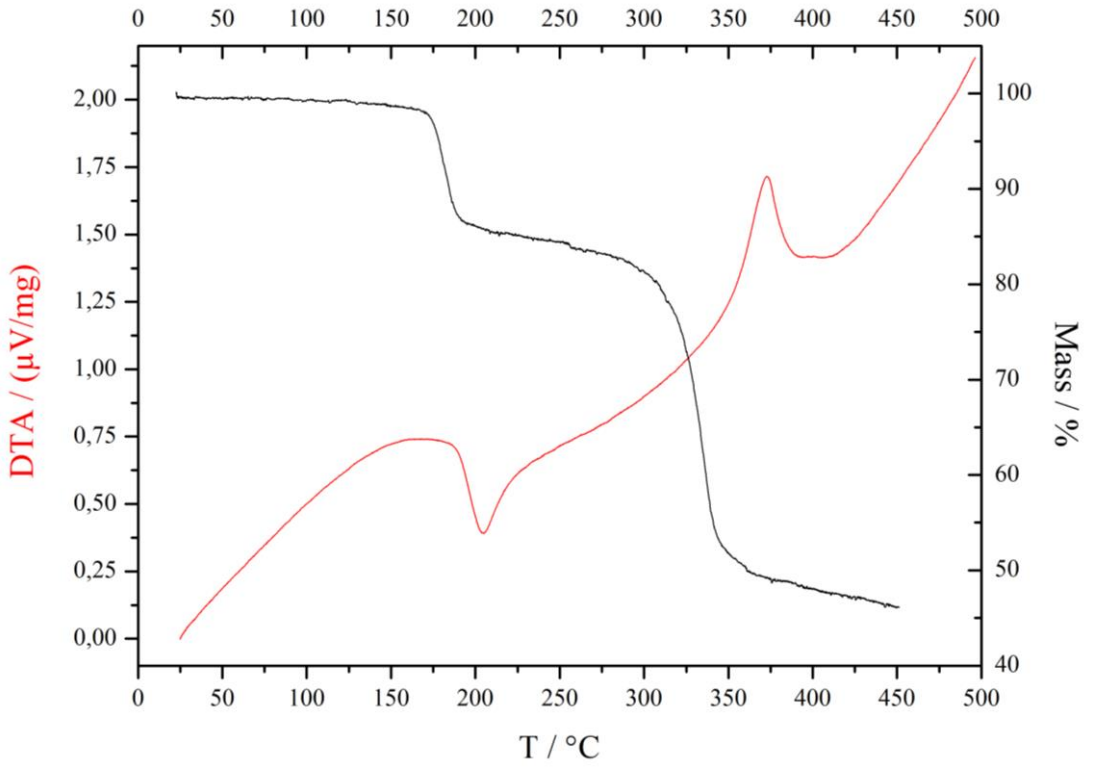

Figure S20: DTA (red) and TG (black) curves of $^{2}_{\infty}[Tm^{III}(tfBDC)(NO_3)(DMSO)_2]$ (**10**).

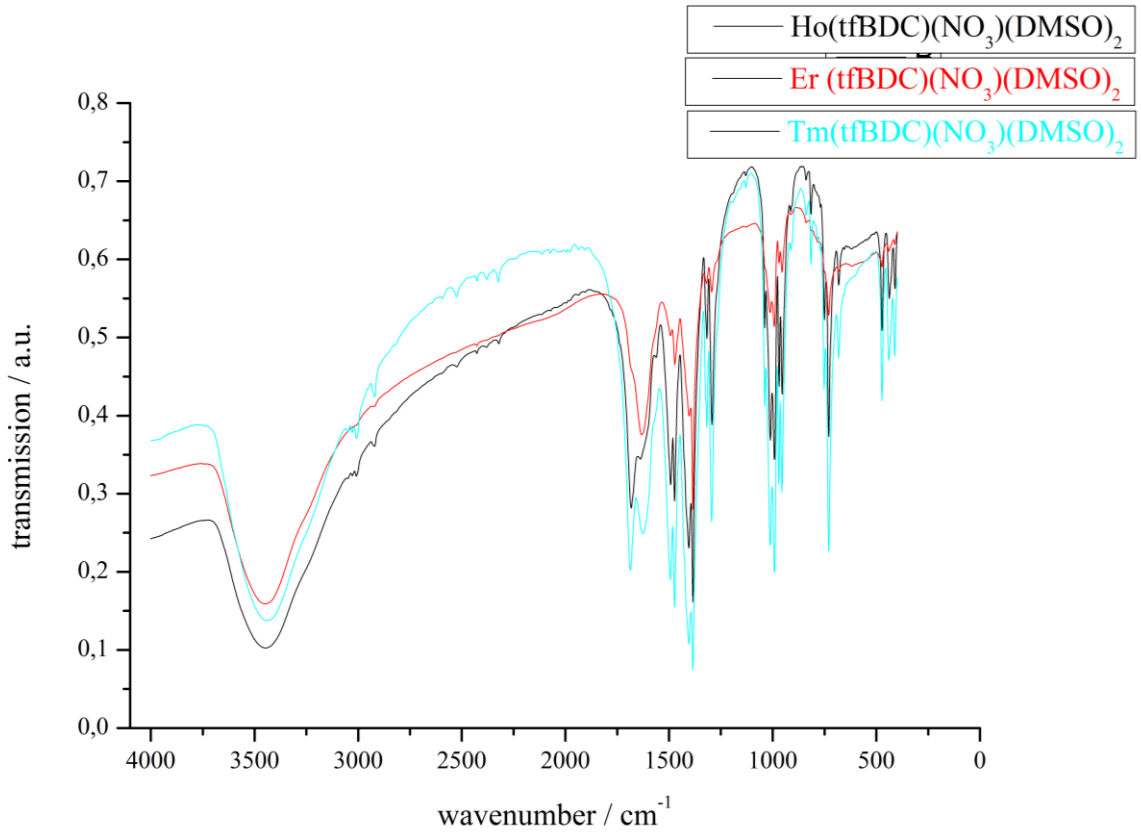

Figure S21: IR spectra of **8** – **10**.

Table S3: Summary of IR data of **8** – **10**.

8	IR (KBr, cm^{-1}): 3448 (b), 3049(w), 3027(w), 3008(w), 2919 (w), 2523(w), 2428(w), 2380(w), 2322 (w), 2114 (w), 2071 (w), 1996 (w), 1936 (w), 1934 (w), 1782 (w), 1682 (m), 1637 (b), 1562 (w), 1491 (m), 1474 (s), 1404 (s), 1385 (s), 1317 (s), 1292 (s), 1128 (w), 1038 (s), 1011 (s), 991 (s), 968 (s), 953 (s), 912 (w), 839 (w), 814 (m), 770 (w), 750 (s), 729 (s), 683 (m), 654 (w), 473 (s), 438 (m), 411 (s).
9	IR (KBr, cm^{-1}): 3448 (b), 3013 (w), 2928 (w), 2428 (w), 2324 (w), 1632 (b), 1493 (w), 1472 (m), 1402 (w), 1385 (s), 1317 (w), 1294 (m), 1038 (w), 1011 (s), 991 (s), 968 (s), 955 (s), 912 (w), 837 (w), 812 (w), 781 (w), 750 (w), 731 (s), 683 (w), 619 (b), 473 (s), 440 (m), 411 (s).
10	IR (KBr, cm^{-1}): 3437 (b), 3049 (w), 3028 (w), 3009 (w), 2920 (w), 2594 (w), 2525 (w), 2426 (w), 2380 (w), 2324 (w), 2112 (w), 2071 (w), 1996 (w), 1978 (w), 1936 (w), 1906 (w), 1686 (m), 1626 (b), 1493 (m), 1474 (s), 1404 (m), 1385 (s), 1317 (s), 1294 (s), 1192 (w), 1128 (w), 1038 (s), 1013 (s), 989 (s). 970 (s), 955 (s), 912 (w), 837 (w), 814 (m), 781 (w), 770 (w), 752 (s), 729 (s), 683 (m), 656 (w), 473 (s), 440 (m), 411 (s).

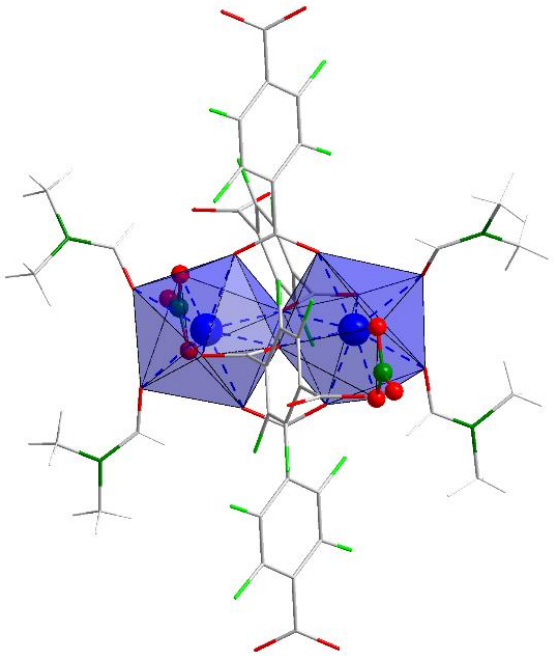

Figure S22: Dimeric units in $^{2}_{\infty}[Eu^{III}(tfBDC)(NO_3)(DMF)_2]\cdot DMF$ (**1**); Eu^{3+} and NO_3^- are shown as balls and sticks, DMF and $tfBDC^{2-}$ are shown as wires/sticks; Eu (blue), O (red), C (light gray), N (green), F (light green), H (white).

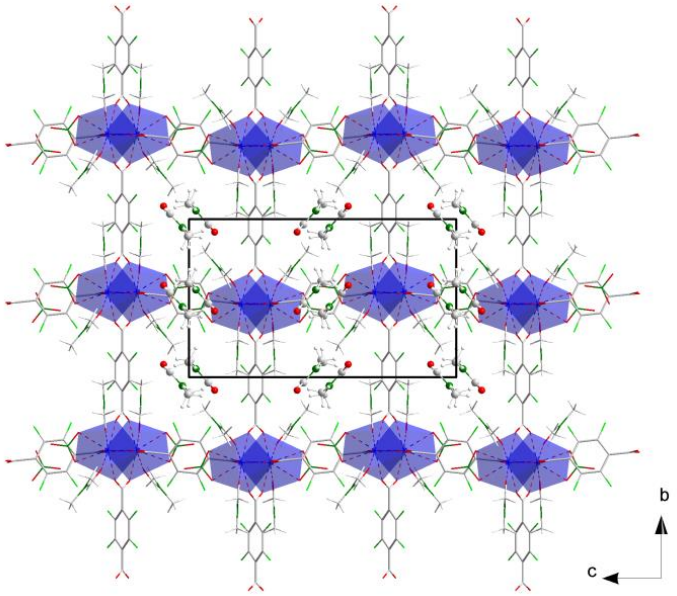

Figure S23: View of a polymeric layer in the crystal structure of $^{2}_{\infty}$ [Eu^{III}(tfBDC)(NO_3)$(DMF)_2$]·DMF (**1**) along [100]; all atoms and bonds are shown in a wires/sticks representation with the exception of non-coordinating DMF molecules (balls and sticks); color coding as in Figure S22.

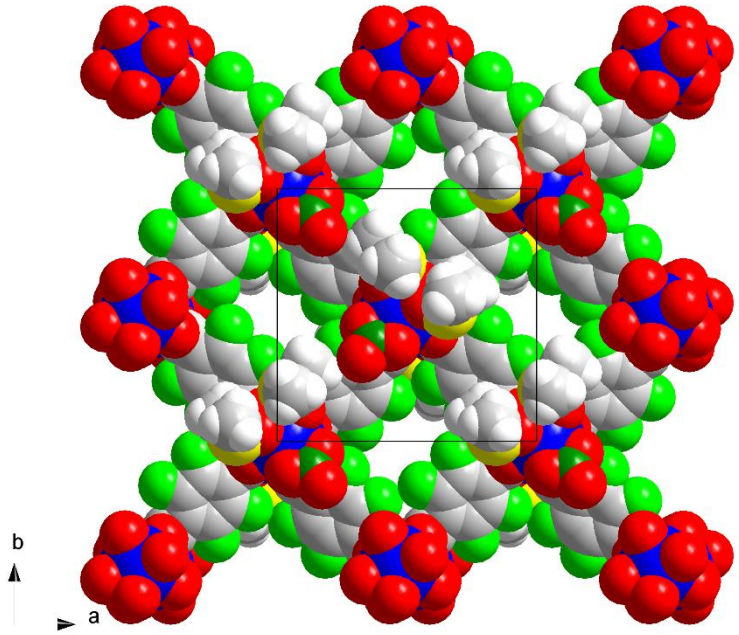

Figure S24: View of a polymeric layer in the crystal structure of $^{2}_{\infty}$ [Tm^{III}(tfBDC)(NO_3)$(DMSO)_2$] (**10**) along [001] in a space-filling presentation; Tm (blue), O (red), C (light gray), N (green), F (light green), S (yellow), H (white).

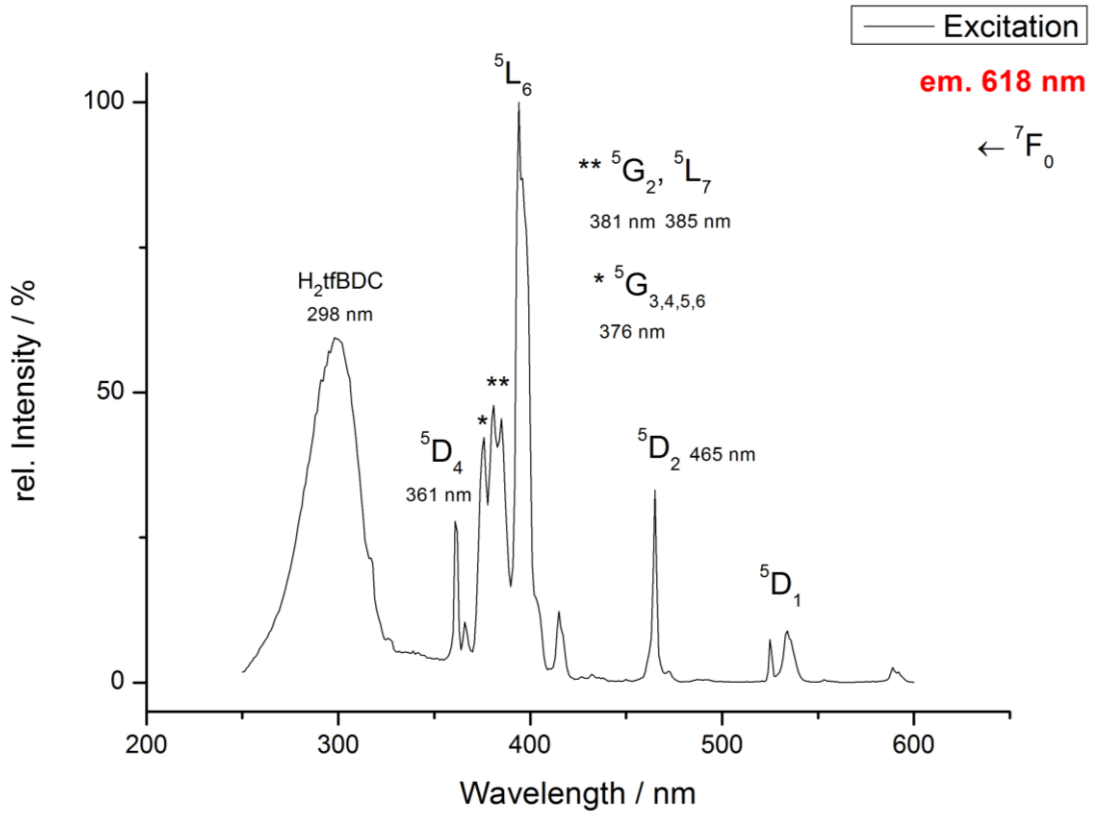

Figure S25: Excitation spectrum of **1**.

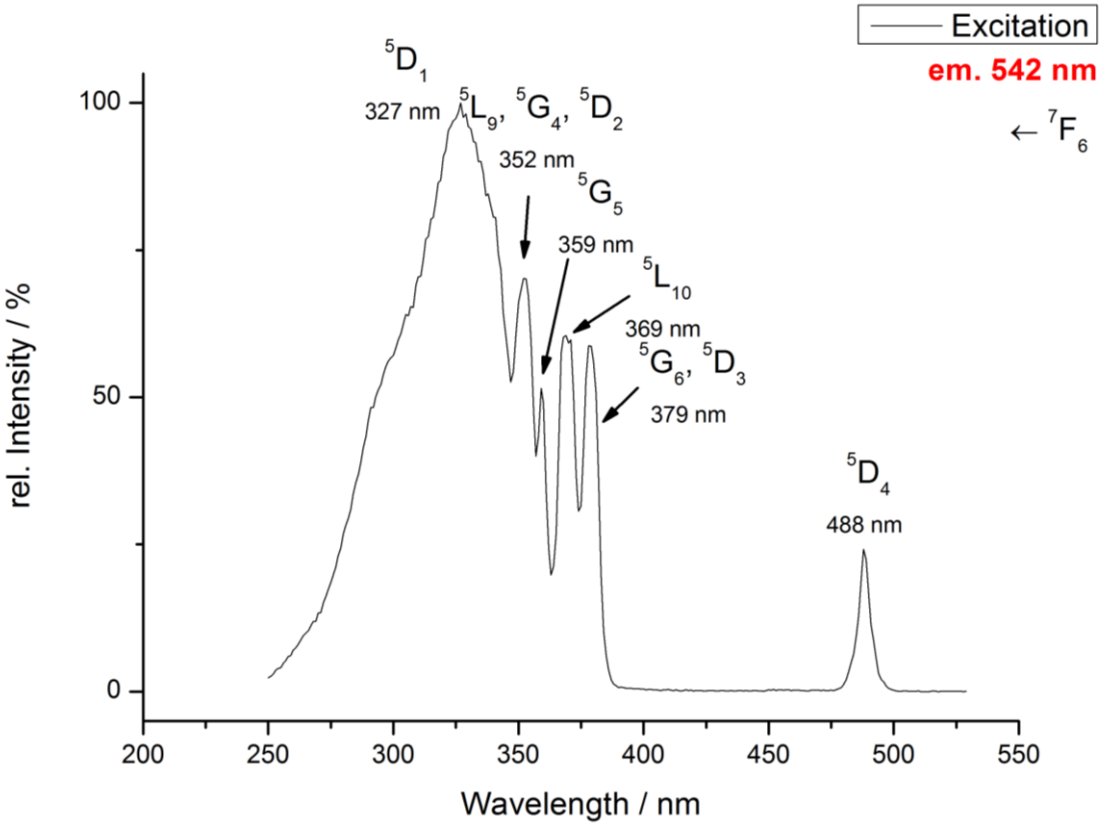

Figure S26: Excitation spectrum of **3**.

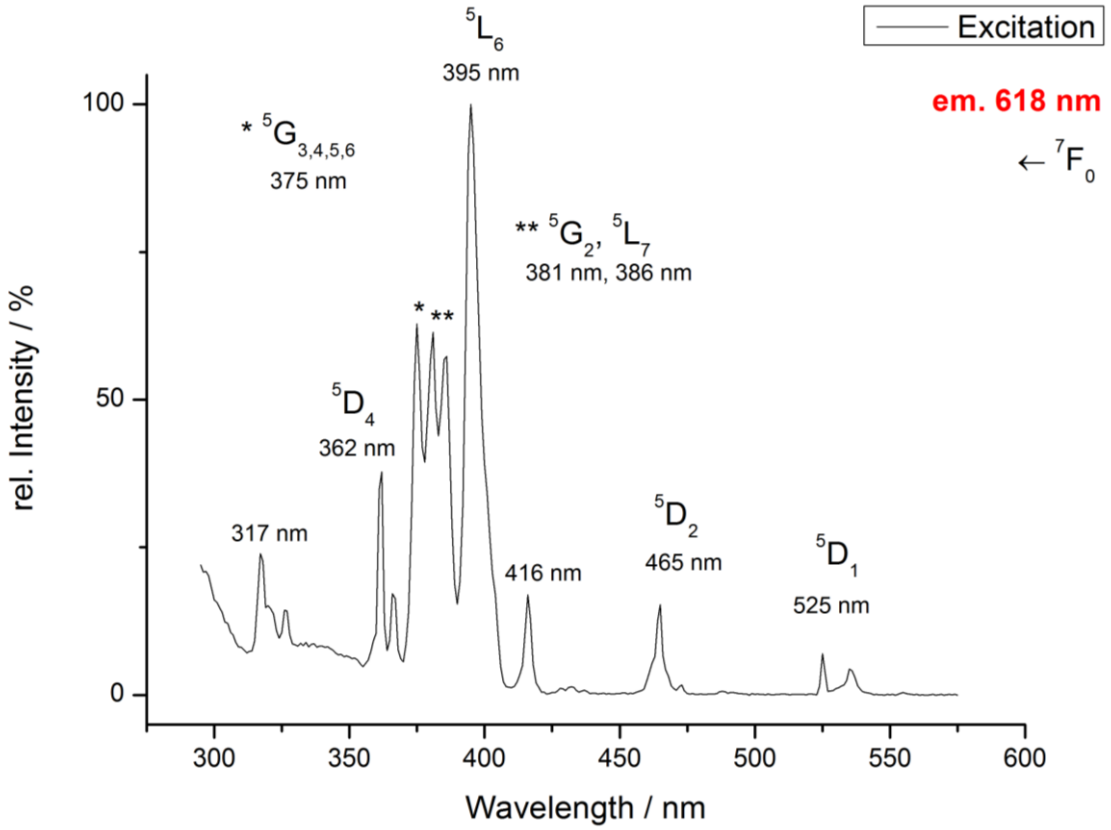

Figure S 27: Excitation spectrum of **7**.

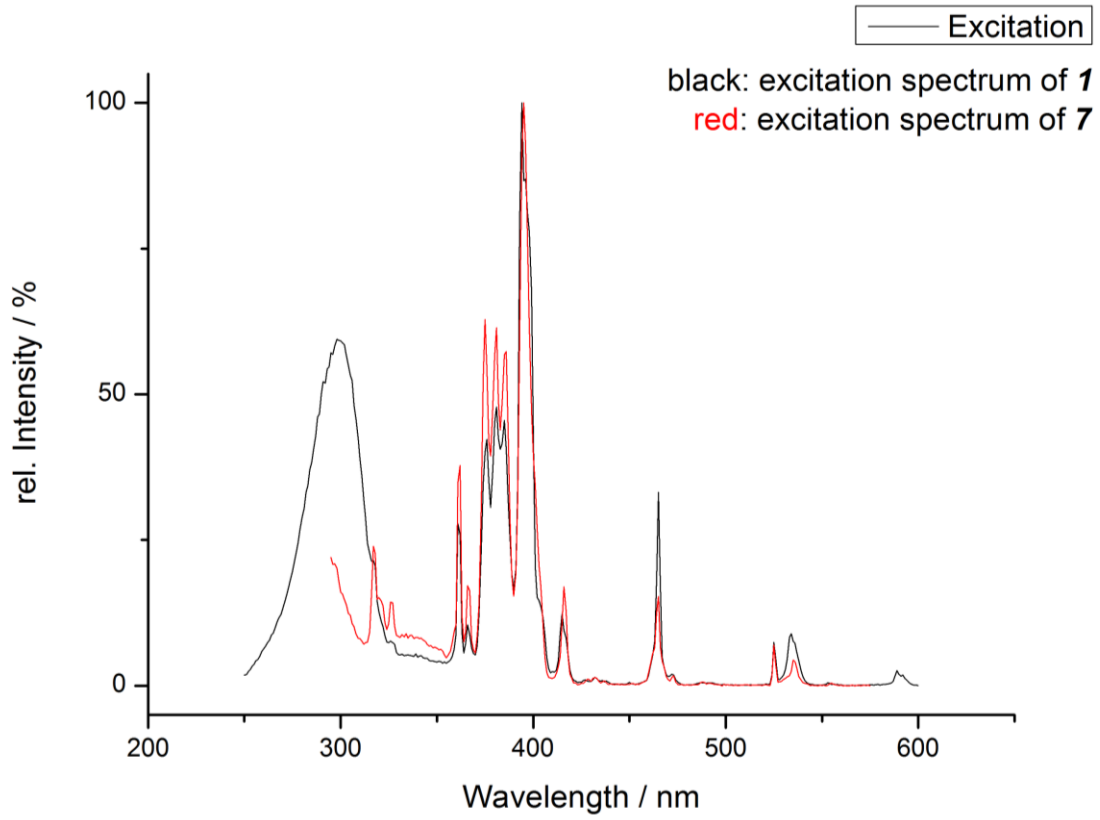

Figure S28: Comparison of excitation spectra of **1** and **7**.

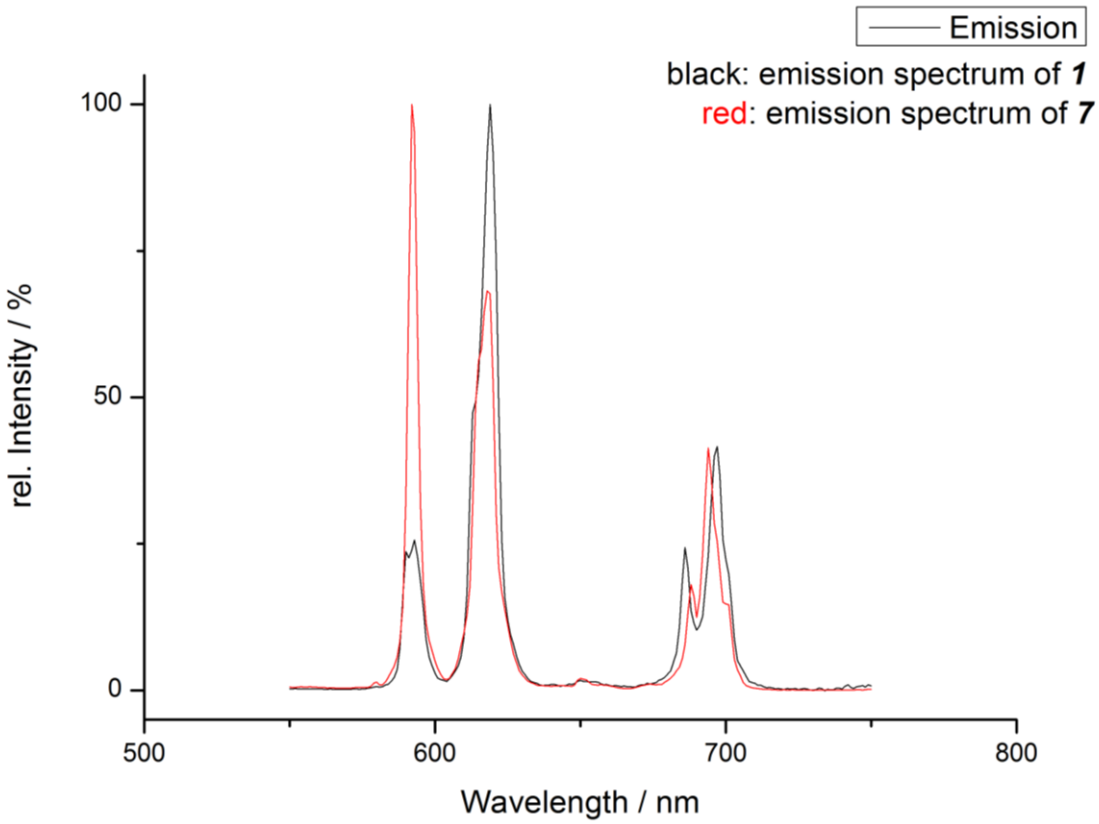

Figure S29: Comparison of emission spectra of **1** and **7**.

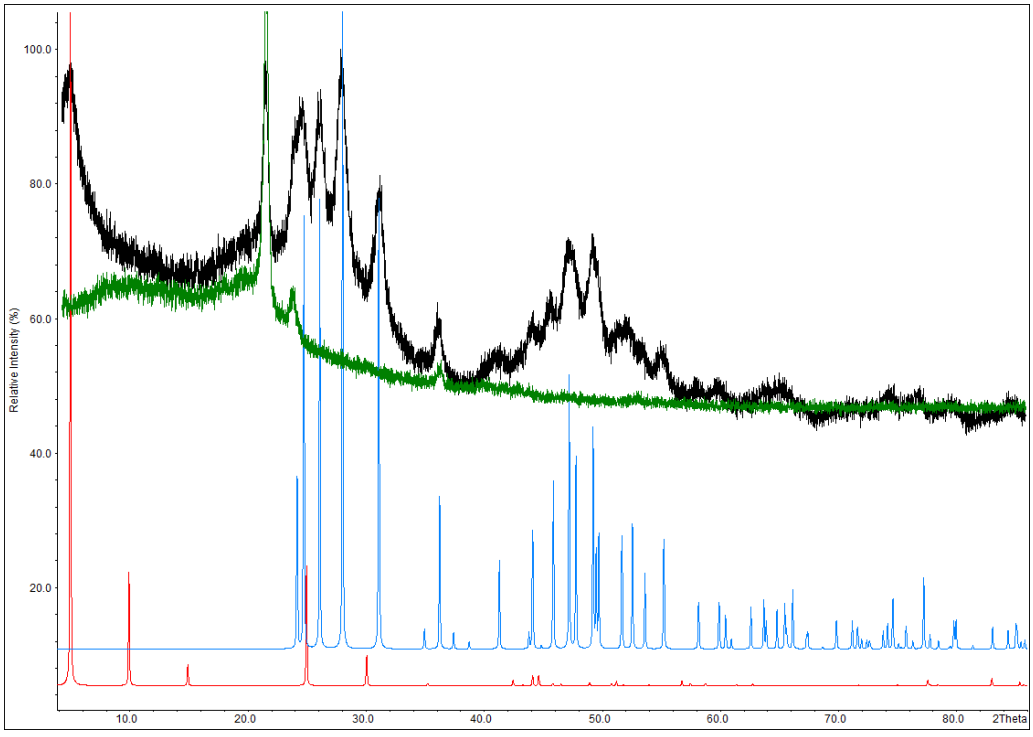

Figure S30: XRPD of the residue of **9** after heating at 500 °C (black curve). The green curve was measured with the empty sample holder (Bragg reflections are due to its transparent foil). Simulated patterns are given for ErF_3 (blue) and rhombohedral graphite (red).